Image Anal Stereol 2026;45: 11-27 doi: 105566/ias.3760
Original Research Paper

MEASUREMENTS OF MUSCLE PHYSIOLOGICAL CROSS-SECTIONAL AREAS OBTAINED BY POINT COUNTING AND METAMORPH

TERESA GARCÍA GARRIDO[1], ANTONIO BLÁZQUEZ ZABALLOS[2], MARÍA ROSA SÁNCHEZ GONZÁLEZ[3], LORENA BENITO GARZÓN✉[,3]

[1]Service de Soins Intermédiaires de Pédiatrie, Hôpital des Enfants, Centre Hospitalier Universitaire Vaudois, Rue de Bugnon 50.1011 Lausanne, Suisse, [2]Departamento de Estadística, Estadística e Investigación Operativa, Facultad de Economía y Empresa, Campus Miguel de Unamuno, Avenida Alfonso X el sabio s/n, Universidad de Salamanca, 37007 Salamanca, España, [3]Departamento de Anatomía e Histología Humanas, Histología Humana, Facultad de Medicina, Avenida Alfonso X el sabio s/n, Universidad de Salamanca, 37007 Salamanca, España

e-mail: teresagag@gmail.com; abz@usal.es; rosan@usal.es; lorenabenito@usal.es

(Received November 22, 2025; revised January 22, 2026; accepted January 27, 2026)

ABSTRACT

Histochemical studies of striated muscles are the most widely used tool for examining their functional properties. The fibres that make up these muscles can be identified by revealing the enzymes involved in contraction, which makes it possible to determine whether they perform resistance (aerobic) or strength (anaerobic) functions. These functions are analysed by comparing the physiological cross-sectional areas of the muscles, regardless of the number of fibres that constitute them or their individual diameters. Areas are measured using an estimated stereological point counting technique in which points are associated with surfaces. This work proposes an automatic, computerised measurement method using the histomorphometric programme Metamorph and compares the results obtained through both methods.

Keywords: histomorphometry, Metamorph, muscle histochemistry, statistics, stereology.

INTRODUCTION

The types of microscopic muscle fibres that make up the striated skeletal muscles of vertebrate animals differ in proportion depending on multiple factors. These types are determined by the neurons that innervate the fibres during their development and are maintained and modified by the activity they perform. In terms of diameter and metabolism, the morphofunctional characteristics of muscle fibres have traditionally been studied and classified based on measurements of their physiological cross-sectional area (PCSA). They have also been classified according to staining results obtained through histochemical methods that reveal enzymes such as myofibrillar adenosine triphosphatase (ATPase) and succinate dehydrogenase (SDH) among the most frequently encountered. PCSA refers to the cross-sectional area occupied solely by muscle fibres, without considering connective tissue or vascularisation. In contrast, the cross-sectional area of a muscle estimates its overall size at a given point and does not accurately reflect the strength capacity of the muscle. Nowadays, tests that provide greater precision in determining fibre type use specific antibodies against different types of myosin molecules; however, they continue to rely on fibre contraction speed and fatigue resistance as firm criteria. The nomenclature for the various fibre types has evolved according to study methodologies and research findings.

In the 1980s, numerous studies examined the composition of limb muscle fibre types in various animal species and in humans. Armstrong and Phelps (1984) described the fibrillar composition of the hindlimb muscles of the rat, using histochemical methods on Sprague–Dawley rats encompassing 98% of the total muscle mass of the rat. They reported 76% fast-twitch glycolytic (FG) fibres, 19% fast-twitch oxidative glycolytic (FOG) fibres, and 5% slow-twitch oxidative (SO) fibres.

In a review, Appell (1988) analysed the possibility of transforming muscle fibres through special training programmes and the significance of muscle biopsies for recognising talent in athletes. The author concluded that the results had been overestimated and were therefore not very significant. Extrapolating the results of studies conducted in other animal species remains a more reliable and ethical approach.

One of the classifications, based on experiments in rats, made it possible to categorise fibres into type

I (slow oxidative), IIA (fast oxidative), IIB (fast glycolytic) and IIX (glycolytic) by studying the tibialis anterior (TA), extensor digitorum longus (EDL) and soleus (SOL) muscles using the ATPase technique with incubation at pH 7.35. The study concluded that the growth process influenced the distribution, proportion, and characteristics of muscle fibre types, and that no IIB fibres were found in the soleus muscle (Konishi *et al.*, 2000).

Studies have also been conducted in rats to determine whether differences exist based on age, sex, and muscle type. Fox *et al.* (2003) found differences in the size of the physiological cross-sectional area of type I, IIA, and IIB fibres. These differences were observed in sex and age and were present in both muscles studied (Fox *et al.*, 2003).

Karen *et al.* (2009) stated that manual identification of muscle fibres in successive serial sections was tedious and time-consuming. In their publication, the authors implemented software to classify and analyse muscle fibre types, thereby avoiding laborious, time-consuming procedures. The authors employed two software programmes (MusRegM and FicClasM) and used human muscle samples (biceps femoris, vastus lateralis and masseter) collected from biopsies and autopsies. Additional samples were obtained from the following rat muscles: extensor digitorum longus, tibialis anterior and gastrocnemius. All samples were frozen in liquid nitrogen and cut serially into 10 µm-thick cross-sections. The expression of myosin heavy chain (MyHC) isoforms and key enzymes involved in the energy supply used in their metabolism was studied. To detect MyHC isoforms, immunohistochemistry was performed using antibodies against myosin heavy chains, including BA-D5 (MyHC-1) and SC-71 (MyHC-2a in rats and MyHC-2a and 2x in humans). The histochemical techniques applied to enzymes were NADH-tetrazolium reductase (NADH-dehydrogenase), succinate dehydrogenase (SDH), and glycerol-3-phosphate dehydrogenase (α-GPDH). Other cryostat sections were processed for in situ hybridisation using specific probes to detect myosin heavy chain (MyHC) transcripts (mRNAs). By using both software programmes and combining classification based on MyHC isoform expression with the activity of energy-producing metabolic enzymes, it was possible to identify oxidative, glycolytic, and oxidative-glycolytic fibres. The authors also conducted semi-quantitative studies of fibre number and proportion.

An innovative technique proposed by Sawano *et al.* (2016) involved the simultaneous use of quadruple immunostaining with antibodies specific for myosin heavy chains (MyHC1, 2A, 2X and 2B) in rats, conjugated to fluorochromes with different excitation and emission wavelengths.

Similar immunohistochemical studies conducted by Bergmeister *et al.* (2017) proposed a simple, fast, automated study protocol using ImageJ, which allowed quantification of the number of fibres via quadruple immunostaining and statistical comparison of the results with manual findings obtained on biceps and lumbrical muscles of rats.

In an immunohistochemical study conducted on hindlimb muscles of kangaroo rats, Ross and Meyers (2021) found a marked predominance of type IIB fibres and a moderate number of type IIA and IIX fibres in all muscles except the soleus.

A method used in our laboratory for measuring surfaces in histological sections is based on the programme Metamorph (Guadilla *et al.*, 2022). The aim of this work was to use this programme to determine the physiological cross-sectional area occupied by each fibre type in the soleus and tibialis anterior muscle sections of Wistar albino rats, using different histochemical techniques for ATPase and SDH. This method is therefore proposed for assessing possible changes in the proportions and percentages of muscle fibres produced by physical exercise.

MATERIALS AND METHODS

To conduct our study, we used a collection of microscope slides generated during the development of an experimental project entitled Muscular changes due to jumping, which was submitted to the competition of the Regional Ministry of Culture and Tourism of Castile and Leon (project number 10.04-542A03.78040.0). This project was selected through a competitive process and involved the Department of Human Anatomy and Histology of the Faculty of Medicine of the University of Salamanca during 2005–2006. The slides selected for this study were those processed with material obtained from 6 Wistar albino rats used as controls.

Histochemical methods

Each muscle fragment was identified by an alphanumeric code consisting of the muscle of origin (S for soleus and T for tibialis anterior) and the laterality of the limb (L for the left side and R for the right).

The histochemical techniques used were the following: ATPase with preincubation at pH 4.9, SDH (succinic dehydrogenase), and ATPase at pH 10.2. For accurate identification of each fragment and the histochemical technique applied, three letters were used: the first capital letter refers to the muscle (‘S’ for soleus and ‘T’ for tibialis anterior), the second capital letter denotes

laterality ('L' for left limb and 'R' for right limb) and the third lower-case letter identifies the technique ('a' for acid ATPase, 'b' for basic ATPase and 's' for SDH).

The histochemical studies were carried out using the technique described by Rivero *et al.* (1996), based on research by Brooke and Kaiser (1970), Schiaffino *et al.* (1989), Gorza (1990) and Santána Pereira *et al.* (1995).

Immunohistochemical techniques allow for more precise muscle fibre typing than histochemical or electrophoresis techniques, especially in the case of fast fibres (Rivero *et al.*, 1996). However, in this work we aimed to study the relative percentage distribution of the areas corresponding to each type of fibre, grouping the categories into the four types proposed according to staining intensity.

Sample selection and analysis

We used a Nikon Coolpix 990 digital camera attached to a Nikon Eclipse 90i microscope with a 4x objective to photograph the most appropriate section on each microscope slide, based on the criteria of transversality and number of fibres. These microphotographs were evaluated to provide a general microscopic description of the most relevant data using Adobe Photoshop 5.5. A grid formed by parallel and perpendicular lines was designed with the computer, defining 17x9 (153) intersection points and delimiting squares. Each intersection point was associated with a point and the area of each square corresponded to the squared length of its side, regardless of the distance between vertices. Since our work is based on percentage points, it was not necessary to define the exact length of the side of the square, which was adapted to allow accurate visual recognition of microscopic images. To determine the respective percentages of each type of fibre for each histochemical technique and each staining intensity grade, the observer used the following formula: the number of points (N) was divided by 153 and the result was multiplied by 100. This percentage was calculated for each image examined in order to compare the results with those obtained using the Metamorph software, following similar identification criteria. We superimposed the 17x9 grid on each photograph to count the intersection points over each type of fibre, following stereological criteria. For each photograph, three counts were performed, selecting the areas of the photograph on which the grid was placed in a systematic random fashion. Subsequently, the arithmetic mean of the three determinations was calculated. As an exclusion criterion, only those points included in a fibre of a specific type that extended into the upper right quadrant were counted.

In all cases of random sampling, a table of random numbers was used.

The images were digitised using the Metamorph Meta Imaging Series 6.1 programme, which facilitates histomorphometric analysis. Variables such as surfaces and perimeters could be measured by quantifying colour differences in the different areas of interest. In this work, only the total surface areas were measured in each case by selecting fibres with similar colour intensity.

In addition, a complete image of the histological section was obtained using a Zeiss Stemi 2000-C loupe equipped with a Zeiss KL1500 electronic light source attached to a Nikon Digital DXm 1200 camera.

The methodology employed in this study, involving stereological criteria, was based primarily on the techniques described by Kroustrup and Gundersen (1983), Gundersen and Jensen (1987), and Gundersen *et al.* (1988).

Statistical assessments of the results were performed using IBM SPSS Statistics version 26. A similar statistical method was used by Staron *et al.* (1999) in their quantitative histochemical studies on the soleus and tibialis anterior muscles of the rat.

RESULTS

Observation of the sections under an optical microscope allowed us to assess the quality of fixation of the muscle fragments. Most of them showed proper fixation, although a small number presented small cavities in the cytoplasm, interpreted as the result of ice crystal formation, which did not invalidate their use.

The muscle fibres generally had a transverse section. Occasionally, areas with transversely sectioned fibres were observed in some samples, alongside other contiguous areas with obliquely sectioned fibres of elliptical or polygonal shape.

The size of the fibres varied. Generally, we found groups of small diameter fibres and other groups of larger diameter fibres, although in both cases the presence of elements of different sizes could not be excluded. These differences in fibre size were very evident in the SDH staining, especially in the tibialis anterior muscle. In this muscle, large unstained fibres, most likely of anaerobic metabolism, could be differentiated from small, most probably aerobic, type I fibres.

Muscle fibre cytoplasm stained by means of ATPase techniques showed homogeneous staining. However, the SDH technique exhibited marked diversity, ranging from intense homogeneous blue staining of the entire surface to little or no staining. In many cases,

fibres presented an intensely stained circular subsarcolemmal rim, while the rest of the circular surface showed little or no staining.

To evaluate these results, the intensity of the individual staining of each fibre was assigned a value: absence of staining was assigned (-), and values (+), (++), or (+++) were assigned depending on the staining intensity from lowest to highest. The microphotographs (Figs. 1–5) show the findings described above.

For counting and measurements using the Metamorph programme, the same area was selected in each microphotograph. The total area of a microphotograph was associated with the number of points it contained: 153 in total. Each point corresponded to the intersection of the vertical and horizontal lines of an overlapping grid. The points were distributed in a pattern in which some were located inside blood vessels or connective tissue, while others were inside the sectioned muscle fibres. Each fibre type was assessed according to standards in stereology, including only those located in the upper right quadrant to avoid counting errors. The area established for counting, measured using Metamorph, had dimensions of 2560 x 1024 pixels, with minimal differences between all the microphotographs studied.

The following tables (Tables 1–3) show the results obtained for each section of each rat. Specifically, each fragment from a different muscle and each technique used is shown. The results include the numerical data of the surface area measured using Metamorph in pixels and the corresponding percentage of surface area estimated by point counting (% area).

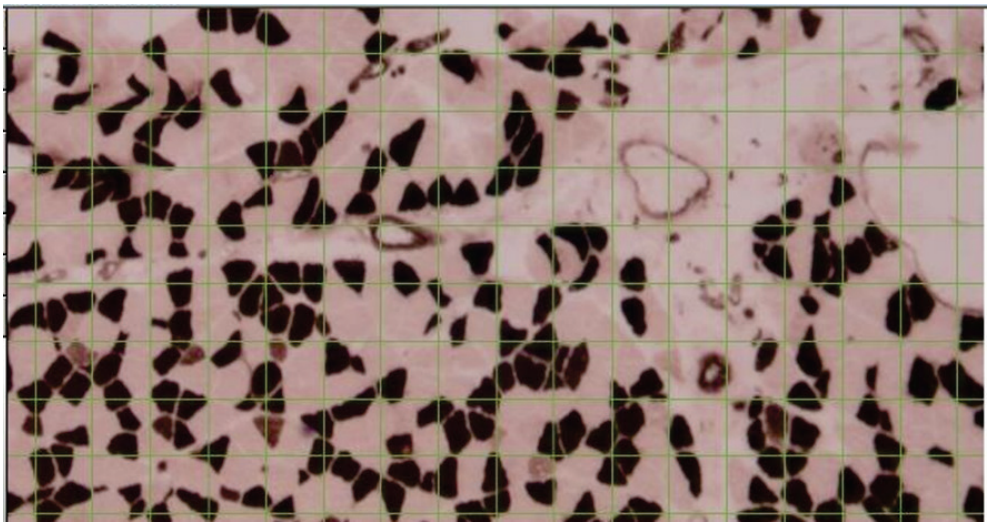

Fig. 1a. *C1 SRb: basic ATPase of the right soleus muscle.*

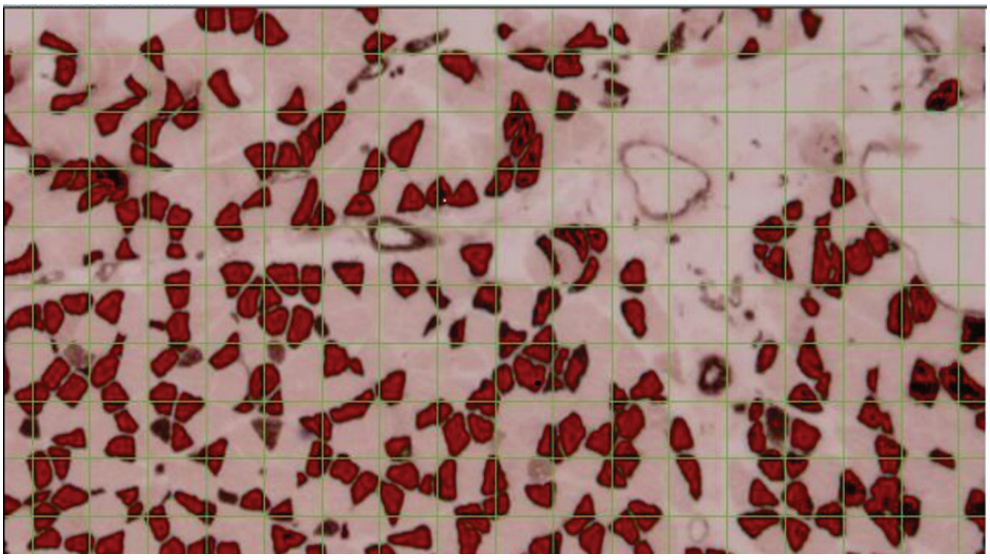

Fig. 1b. *C1 SRb +++: basic ATPase of the right soleus muscle. In red colour, the fibres stained with the highest intensity (+++) identified using Metamorph.*

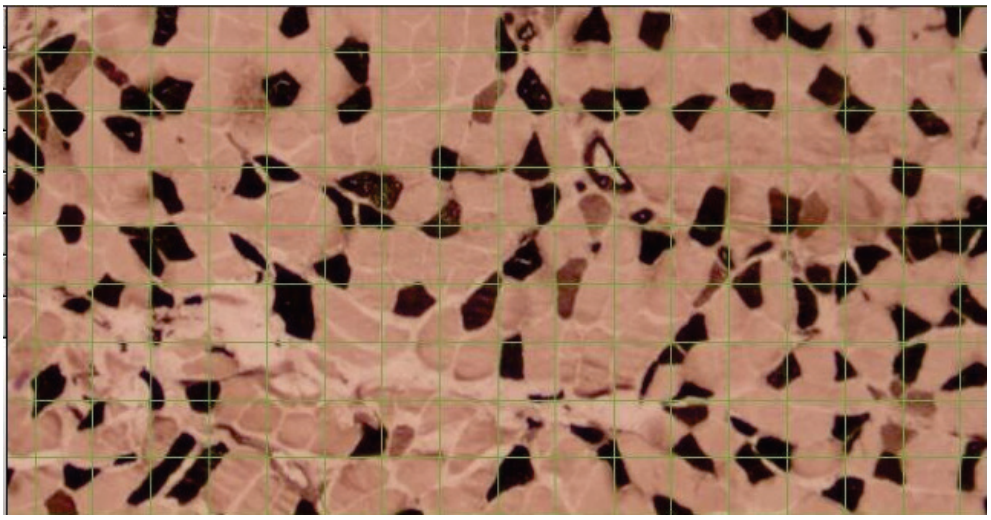

Fig. 2a. *C2 SLa: acid ATPase of the left soleus muscle.*

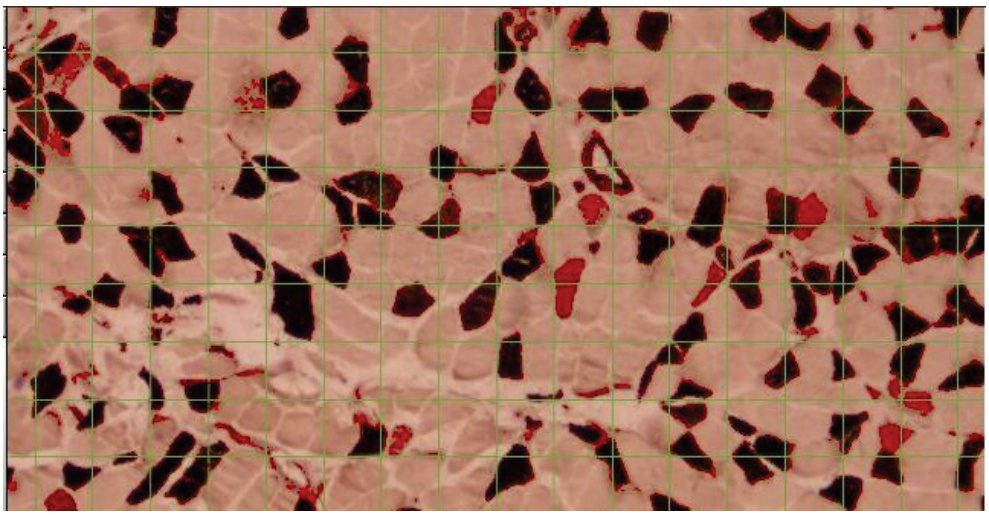

Fig. 2b. *C2 SLa ++: acid ATPase of the left soleus muscle. In red colour, the fibres stained with moderate intensity (++) identified using Metamorph.*

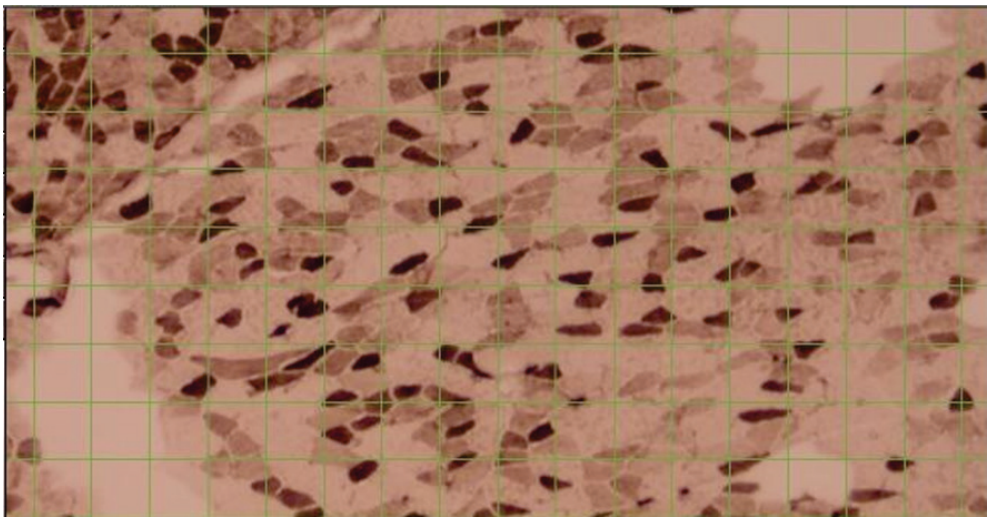

Fig. 3a. *C2 TLb: basic ATPase of the left tibialis anterior muscle.*

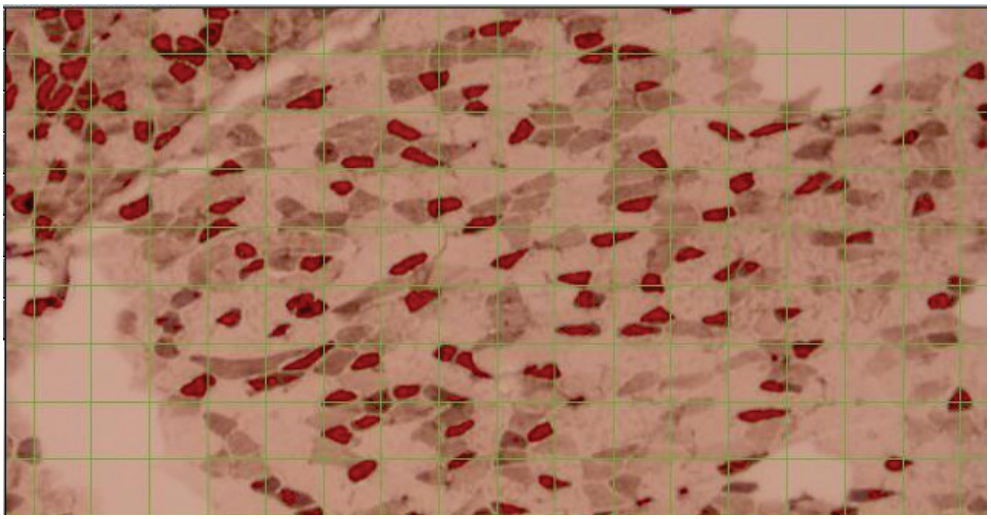

Fig. 3b. *C2 TLb +++: basic ATPase of the left tibialis anterior muscle. In red colour, the fibres stained with the highest intensity (+++) identified using Metamorph.*

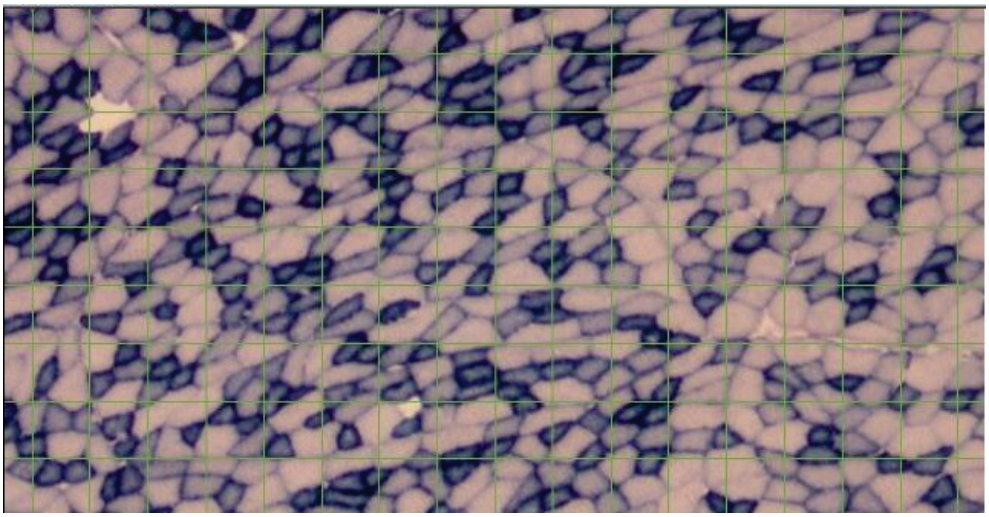

Fig. 4a. *C2 TLs: SDH of the left tibialis anterior muscle.*

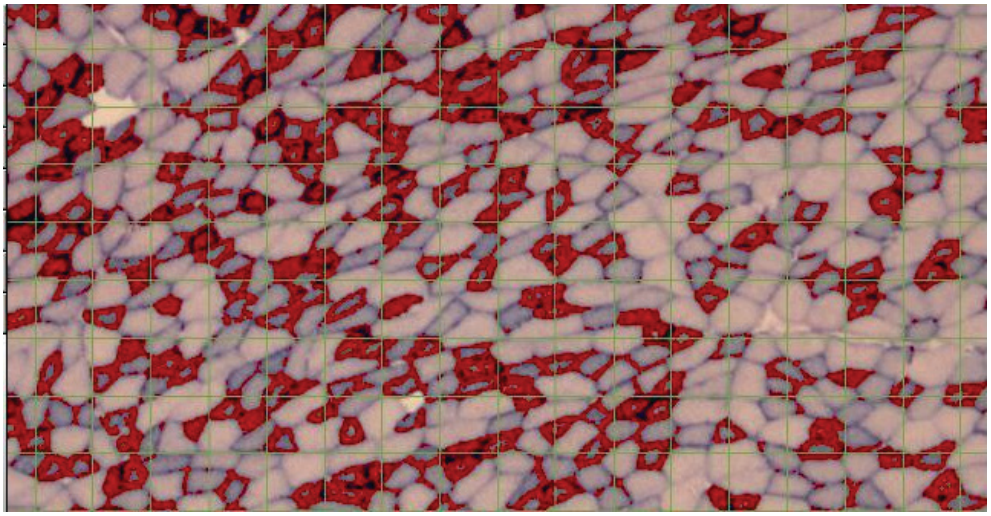

Fig. 4b. *C2 TLs +++: SDH of the left tibialis anterior muscle. In red colour, the fibres stained with the highest intensity (+++) identified using Metamorph.*

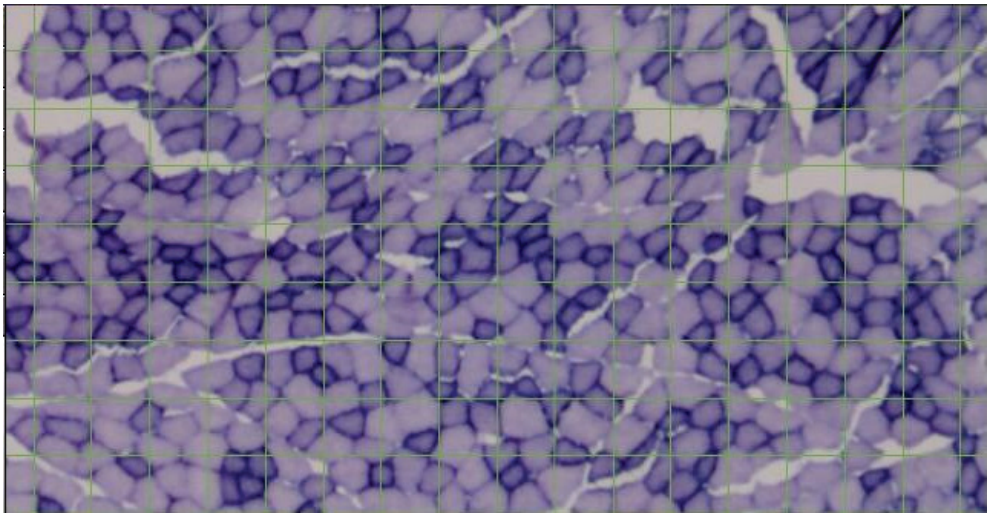

Fig. 5a. *C5 TLs: SDH of the left tibialis anterior muscle.*

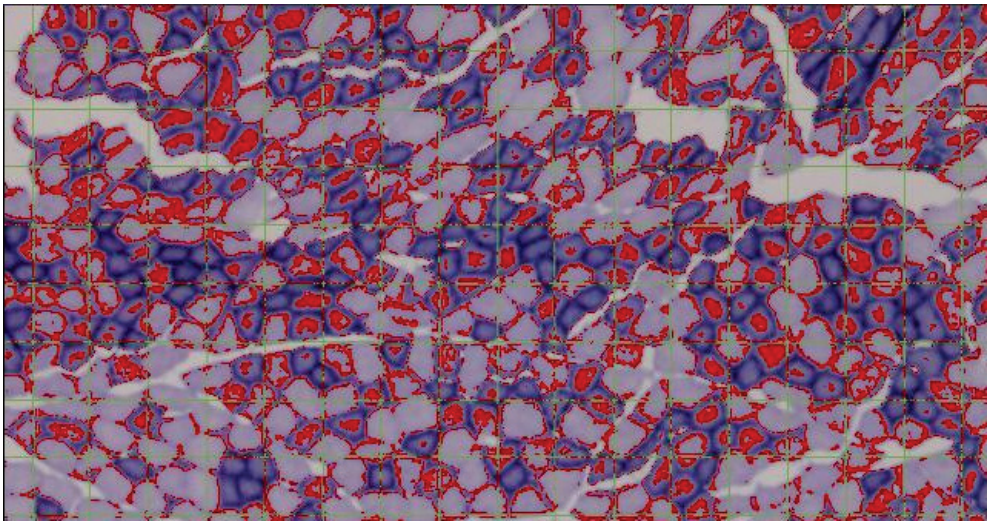

Fig. 5b. *C5 TLs ++: SDH of the left tibialis anterior muscle. In red colour, fibres with moderate intensity (++) identified using Metamorph.*

Table 1. *Results with the acid ATPase technique.*

Rat	**SLa +++** (pixels)	**SLa +++** (% area)	**SLa ++** (pixels)	**SLa ++** (% area)	**SLa +** (pixels)	**SLa +** (% area)	**SLa –** (pixels)	**SLa –** (% area)
1	0	0	67049	30.03	116025	51.97	0	0
2	0	0	45243	19.87	146061	64.17	0	0
3	0	0	53793	23.69	166567	73.36	0	0
4	0	0	51807	23.14	88189	39.40	0	0
5	0	0	73310	32.56	119670	53.15	0	0
6	0	0	69744	31.25	111350	49.89	0	0

Rat	**SRa +++** (pixels)	**SRa +++** (% area)	**SRa ++** (pixels)	**SRa ++** (% area)	**SRa +** (pixels)	**SRa +** (% area)	**SRa –** (pixels)	**SRa –** (% area)
1	0	0	48489	21.63	72698	32.43	75584	33.71
2	0	0	42429	18.79	143850	63.71	0	0
3	31381	13.85	62250	27.48	0	0	0	0
4	0	0	87296	38.6	91568	40.49	0	0
5	0	0	42027	18.45	82292	36.14	0	0
6	0	0	41778	18.53	137215	60.89	0	0
Rat	**TLa +++** (pixels)	**TLa +++** (% area)	**TLa ++** (pixels)	**TLa ++** (% area)	**TLa +** (pixels)	**TLa +** (% area)	**TLa –** (pixels)	**TLa –** (% area)
1	0	0	96782	42.85	16130	7.14	0	0
2	0	0	158905	71.16	0	0	0	0
3	0	0	150641	67.31	29250	13.06	0	0
4	0	0	155410	68.94	11910	5.28	0	0
5	0	0	136058	60.69	0	0	0	0
6	0	0	152127	68.36	0	0	0	0

Rat	**TRa +++** (pixels)	**TRa +++** (% area)	**TRa ++** (pixels)	**TRa ++** (% area)	**TRa +** (pixels)	**TRa +** (% area)	**TRa –** (pixels)	**TRa –** (% area)
1	0	0	136287	61.86	10234	4.64	0	0
2	0	0	146390	65.02	41424	18.4	0	0
3	0	0	115110	51.43	36610	16.35	0	0
4	0	0	159991	71.48	0	0	0	0
5	0	0	138513	61.02	0	0	0	0
6	0	0	146693	64.99	0	0	0	0

Table 2. *Results with the basic ATPase technique.*

Rat	**SLb +++** (pixels)	**SLb +++** (% area)	**SLb ++** (pixels)	**SLb ++** (% area)	**SLb +** (pixels)	**SLb+** (% area)	**SLb –** (pixels)	**SLb –** (% area)
1	45520	20.27	16577	7.38	91565	70	0	0
2	39926	17.15	19449	8.55	123492	93	0	0
3	39967	17.63	14706	6.48	101699	86	0	0
4	8823	3.89	51463	22.7	136663	85	0	0
5	10588	4.71	23409	10.42	118721	84	0	0
6	23520	10.4	2647	1.17	115667	99	0	0

Rat	**SRb +++** (pixels)	**SRb +++** (% area)	**SRb ++** (pixels)	**SRb ++** (% area)	**SRb +** (pixels)	**SRb +** (% area)	**SRb –** (pixels)	**SRb –** (% area)
1	20166	8.99	8453	3.77	0	0	75584	33.71
2	28066	12.41	15348	6.78	118648	52.48	0	0
3	20284	9.06	16346	7.30	97244	43.45	0	0
4	9714	4.31	49488	21.98	99929	44.39	0	0
5	26843	11.75	4447	1.94	90685	39.71	0	0
6	41726	18.6	16338	7.28	119137	53.13	0	0
Rat	**TLb +++** (pixels)	**TLb +++** (% area)	**TLb ++** (pixels)	**TLb ++** (% area)	**TLb +** (pixels)	**TLb +** (% area)	**TLb –** (pixels)	**TLb –** (% area)
1	0	0	83695	37.12	0	0	6737	2.98
2	10461	4.69	36043	16.17	0	0	124711	55.97
3	0	0	110585	49.69	5523	24.82	2146	0.96
4	71116	31.45	134332	59.42	6608	2.92	0	0
5	0	0	113818	49.94	0	0	0	0
6	0	0	13509	60.54	0	0	0	0

Rat	**TRb +++** (pixels)	**TRb +++** (% area)	**TRb ++** (pixels)	**TRb ++** (% area)	**TRb +** (pixels)	**TRb +** (% area)	**TRb –** (pixels)	**TRb –** (% area)
1	0	0	126887	57.75	72907	33.18	0	0
2	4326	1.92	36905	16.44	146989	65.49	0	0
3	0	0	152061	68.61	2483	1.12	0	0
4	44086	19.5	0	0	132276	56.51	11625	5.14
5	2003	0.88	126780	56.06	0	0	0	0
6	0	0	143464	64.0	0	0	0	0

Table 3. *Results with the SDH technique.*

Rat	SLs +++ (pixels)	SLs +++ (% area)	SLs ++ (pixels)	SLs ++ (% area)	SLs + (pixels)	SLs + (% area)	SLs – (pixels)	SLs – (% area)
1	58122	26.05	0	0	104582	46.87	0	0
2	41593	18.39	0	0	94955	42.03	0	0
3	0	0	42529	18.93	57718	25.7	0	0
4	0	0	95178	41.81	76187	33.47	0	0
5	49145	21.89	79007	35.2	80745	35.97	0	0
6	85158	38.32	69888	31.45	0	0	0	0

Rat	SRs +++ (pixels)	SRs +++ (% area)	SRs ++ (pixels)	SRs ++ (% area)	SRs + (pixels)	SRs + (% area)	SRs – (pixels)	SRs – (% area)
1	69497	31.01	77301	34.49	0	0	0	0
2	88261	39.43	0	0	121779	54.41	0	0
3	72642	31.67	41792	18.22	19745	8.61	0	0
4	0	0	121567	54.13	48084	21.36	0	0
5	86640	38.36	86539	38.31	0	0	0	0
6	81808	36.84	0	0	104131	46.89	0	0

Rat	TLs +++ (pixels)	TLs +++ (% area)	TLs ++ (pixels)	TLs ++ (% area)	TLs + (pixels)	TLs + (% area)	TLs – (pixels)	TLs – (% area)
1	61997	27.78	0	0	57270	25.66	0	0
2	39615	17.56	0	0	67385	29.87	62664	27.78
3	64611	28.33	94947	41.63	34964	15.33	0	0
4	0	0	77815	34.81	122955	55.0	0	0
5	65865	28.96	23258	10.22	108607	47.75	0	0
6	35525	15.8	0	0	156518	69.62	0	0

Rat	TRs +++ (pixels)	TRs +++ (% area)	TRs ++ (pixels)	TRs ++ (% area)	TRs + (pixels)	TRs + (% area)	TRs – (pixels)	TRs – (% area)
1	96452	42.51	0	0	30171	13.3	0	0
2	67934	30.13	53948	23.53	73965	32.81	0	0
3	75363	33.75	93069	4.69	0	0	0	0
4	49106	21.43	54235	23.67	61937	27.03	0	0
5	50942	22.89	20716	12.9	75203	33.78	0	0
6	61934	27.55	31174	13.86	81385	36.2	0	0

DISCUSSION

A repeated measures model was used to compare the percentages obtained from both methods. The measurements corresponded to assessments carried out using the point counting method on the one hand and the Metamorph surface area on the other. In the model used to compare both methods in each technique (acid, basic and SDH), the following three factors were considered: muscle with two levels (soleus and tibialis anterior), side with two levels (left and right), and intensity with four levels ('-', '+', '++' and '+++'). Levene's test was conducted to assess the homogeneity of variances.

ACID (acid ATPase technique)

In the analysis of the statistical model for acid ATPase, the absent (-) and highest (+++) intensities were excluded. In the absence of staining, variability was zero, as all observed data were equal to zero. At the highest intensities, a similar pattern occurred in most muscle and side combinations (left soleus, left tibialis anterior, and right tibialis anterior). Homogeneity of variances was observed: the p-value obtained in Levene's test for point counting (ratio %) was 0.136, and the p-value for Metamorph surface area (%) was 0.073.

In the saturated model, which included all possible two- and three-way interactions, the triple interaction 'Muscle*Side*Intensity' (p-value = 0.838) and the double interactions 'Side*Intensity' (p-value = 0.310) and 'Muscle*Side' (p-value = 0.149) were not significant. Conversely, the double interaction 'Muscle*Intensity' was highly significant (p-value = 0.000000139).

In the model resulting from the analysis, the non-significant interaction effects were excluded, but the main effects of the principal factors ('Muscle', 'Side', and 'Intensity') were retained. In addition, the double interaction effect 'Muscle*Intensity' was found to be significantly non-zero. The estimate of the common variance using this model was 4.568 ($\hat{s}_D$).

Table 4 and Fig. 6 show the mean percentages calculated by point counting (ratio %) and Metamorph surface area (%) in each of the 16 combinations of Muscle, Side, and Intensity.

At the moderate intensity (++), significantly different percentage means for point counting and Metamorph surface area were observed in both muscles and both sides. This occurred in all Muscle–Side combinations except for the left soleus. In all cases, the Metamorph surface area percentages were significantly lower than the point counting percentages, with the previously mentioned exception of the left soleus.

At the remaining intensities, significantly different percentage means for point counting and Metamorph surface area were observed only at the low intensity (+) of the right soleus, where the mean percentage calculated through Metamorph surface area was significantly lower than the mean percentage obtained by point counting.

BASIC (basic ATPase technique)

Homogeneity of variances was observed, as the p-values obtained from Levene's test were 0.062 for point counting (%) and 0.051 for Metamorph surface area (%).

The triple interaction 'Muscle*Side*Intensity' (p-value = 0.668), and the double interactions 'Muscle*Side' (p-value = 0.433) and 'Side*Intensity' (p-value = 0.867) were not significant. Conversely, the double interaction 'Muscle*Intensity' was highly significant (p-value = 0.0000002).

In the model resulting from the analysis, the non-significant interaction effects were excluded. The model included the main effects of each of the factors ('Muscle', 'Side' and 'Intensity') and the significant double interaction effect 'Muscle*Intensity'. The estimate of the common variance with this model was 5.377 ($\hat{s}_D$).

Table 4. *Mean sample values for point counting and Metamorph surface area in each of the 16 combinations of Muscle, Side, and Intensity in the acid ATPase technique. Asterisks (*) indicate a significant difference between the percentages calculated from point counting (ratio %) and those obtained from Metamorph surface area (%) (* $p < 0.05$).*

Muscle	*Side*	*Intensity*		*Point counting (ratio %)*	*Metamorph surface area (%)*
Soleus	Left	"+++"		0	0
		"++"		25.16	26.76
		"+"		58.28	55.32
		"-"		0	0
	Right	"+++"		3.49	2.31
		"++"	*	31.05	23.91
		"+"	*	46.08	38.94
		"-"		0	0
Anterior Tibial	Left	"+++"		1.42	0
		"++"	*	81.15	63.22
		"+"		2.51	4.25
		"-"		0	0
	Right	"+++"		0	0
		"++"	*	83.12	62.63
		"+"		4.36	6.57
		"-"		0	0

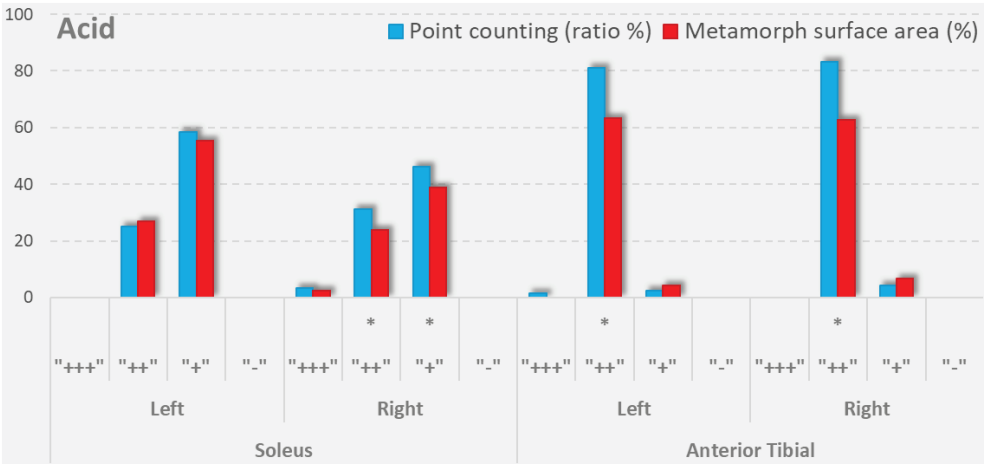

Fig. 6. *Mean sample values for point counting and Metamorph surface area in each of the 16 combinations of Muscle, Side, and Intensity in the acid ATPase technique. Asterisks (*) indicate a significant difference between the percentages calculated from point counting (ratio %) and those obtained from Metamorph surface area (%) (* $p < 0.05$).*

Table 5 and Fig.7 below show the mean percentages for point counting (ratio %) and Metamorph surface area (%) across all combinations of Muscle, Side, and Intensity.

Table 5. *Sample mean values for point counting and Metamorph surface area in each of the 16 combinations of Muscle, Side, and Intensity in the basic ATPase technique. Asterisks (*) indicate a significant difference when comparing the percentages calculated from point counting (ratio %) with those obtained from Metamorph surface area (%) (* p < 0.05).*

Muscle	*Side*	*Intensity*		*Point counting (ratio %)*	*Metamorph surface area (%)*
Soleus	Left	"+++"	*	21.9	12.34
		"++"		6.32	9.45
		"+"		56.32	50.5
		"-"		0	0
	Right	"+++"	*	20.37	10.85
		"++"		6.21	8.18
		"+"		43.46	38.86
		"-"		7.3	5.62
Anterior Tibial	Left	"+++"		7.19	6.02
		"++"	*	62.85	45.48
		"+"		2.07	4.62
		"-"		10.24	9.99
	Right	"+++"		3.92	3.72
		"++"	*	53.81	43.81
		"+"		24.73	26.05
		"-"		0	0.86

At the highest intensity (+++), the mean point counting percentages in the soleus muscles on both sides were significantly higher than the corresponding Metamorph surface area percentages. However, in the tibialis anterior muscles on both sides, the mean point counting and Metamorph surface area percentages showed only minor, non-significant differences.

At the moderate intensity (++), the tibialis anterior muscles on both sides showed mean point counting percentages that were significantly higher than the corresponding Metamorph surface area percentages. In the left soleus muscle, the mean point counting percentages were significantly lower than the corresponding Metamorph surface area percentages. The differences were not significant in the right soleus muscle.

At the absent (-) and low (+) intensities, the differences were minimal and not significant in all four muscle–side combinations.

SDH (Succinate dehydrogenase technique)

For the analysis of the SDH technique, the absent intensity (-) was excluded because it showed no variability, as all the data obtained were zero.

Homogeneity of variances was observed, with p-values obtained from Levene's test being 0.103 for point counting (%) and 0.424 for Metamorph surface area (%).

The triple interaction 'Muscle*Side*Intensity' (p-value = 0.075) and the double interaction 'Muscle*Side' (p-value = 0.294) were not significant. Conversely, the double interactions 'Muscle*Intensity' (p-value = 0.016) and 'Side*Intensity' (p-value = 0.019) were significant.

The model resulting from the analysis was the one in which non-significant interaction effects were excluded. The model included the main effects of the factors 'Muscle', 'Side', and 'Intensity', as well as the significant double interaction effects 'Muscle*Intensity' and 'Side*Intensity'. The estimate of the common variability with this model was 7.98 ($\hat{s}_D$).

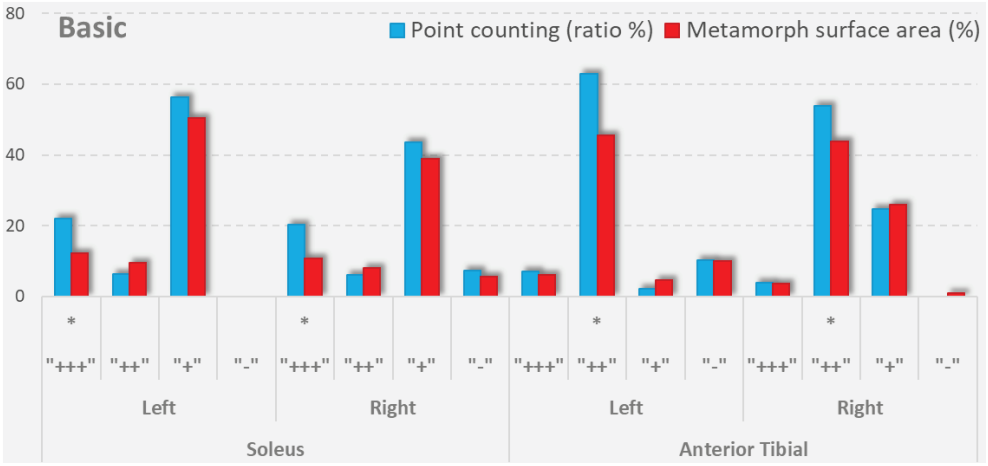

Fig. 7. *Sample mean values for point counting and Metamorph surface area in each of the 16 combinations of Muscle, Side, and Intensity in the basic ATPase technique. Asterisks (*) indicate a significant difference when comparing the percentage values calculated from point counting (ratio %) with those obtained from Metamorph surface area (%) (* p < 0.05).*

Table 6 and Fig.8 show the average values of the percentages calculated for point counting (ratio %) and Metamorph surface area (%) for all combinations of Muscle, Side, and Intensity.

Table 6. *Sample mean values for point counting and Metamorph surface area in each of the 16 combinations of Muscle, Side, and Intensity in the SDH technique. Asterisks (*) indicate a significant difference when comparing the percentage values calculated from point counting (ratio %) with those obtained from Metamorph surface area (%) (* p < 0.05).*

Muscle	*Side*	*Intensity*		*Point counting (ratio %)*	*Metamorph surface area (%)*
Soleus	Left	"+++"	*	26.47	17.44
		"++"	*	46.51	36.05
		"+"		14.16	15.86
		"-"		0	0
	Right	"+++"		26.03	29.55
		"++"		37.15	34.76
		"+"		20.04	14.06
		"-"		0	0
Anterior Tibial	Left	"+++"		28	19.74
		"++"		10.68	14.44
		"+"		40.2	40.54
		"-"		9.48	4.63
	Right	"+++"		36.17	29.71
		"++"		15.58	13.11
		"+"		32.14	23.85
		"-"		0	0

Significant differences were found only in the left soleus at the highest (+++) and moderate (++) intensities when comparing the mean values for point counting (ratio %) and Metamorph surface area (%).

To compare surface area percentages, a model was used in each technique (acid, basic and SDH) in which three factors were considered: Muscle with two levels (soleus and tibialis anterior), Side with two levels (left and right) and Intensity with four levels ('-', '+', '++' and '+++'). As before, to statistically evaluate the model, intensities with no variability were excluded. Therefore, in the acid and basic ATPase techniques, the absent (-) and highest (+++) intensities were excluded. In the SDH technique, the absent (-) intensity was excluded. The average percentages are shown in Figs. 9, 10, and 11.

Fig. 9 shows the acid ATPase results. It should be noted that in the soleus, the average surface area percentage for the light intensity (+) was significantly higher than that for the moderate intensity (++). However, this pattern was reversed in the tibialis anterior muscle, where the average surface area percentage for the moderate intensity (++) was significantly higher than that for the light intensity (+). Fig. 9 also shows that no significant differences in the average surface area percentage were found when comparing the left and right sides in any muscle–intensity combination.

Fig. 10 shows the results of the basic ATPase technique. As already described for the acid ATPase technique, it can be observed that in the case of the soleus the average surface area percentage for the light intensity (+) was significantly higher than that for the moderate intensity (++). However, this pattern was reversed in the tibialis anterior muscle, where the average surface area percentage for the moderate intensity (++) was significantly higher than that for the light intensity (+). Fig. 10 also shows that there were no significant differences in the average surface area percentage between the left and right sides in any muscle–intensity combination, except for the tibialis anterior muscle at the light intensity (+).

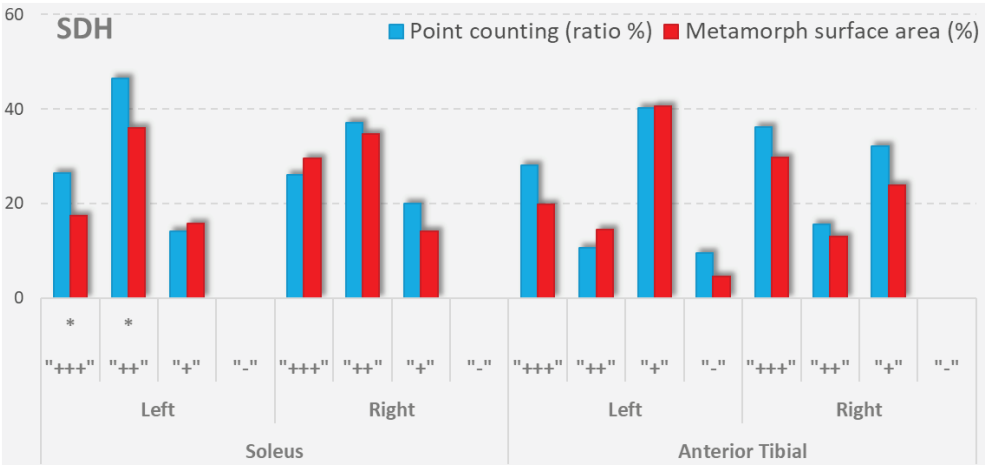

Fig. 8. *Sample mean values for point counting and Metamorph surface area in each of the 16 combinations of Muscle, Side, and Intensity in the SDH technique. Asterisks (*) indicate a significant difference when comparing the percentage values calculated from point counting (ratio %) with those obtained from Metamorph surface area (%) (* p < 0.05).*

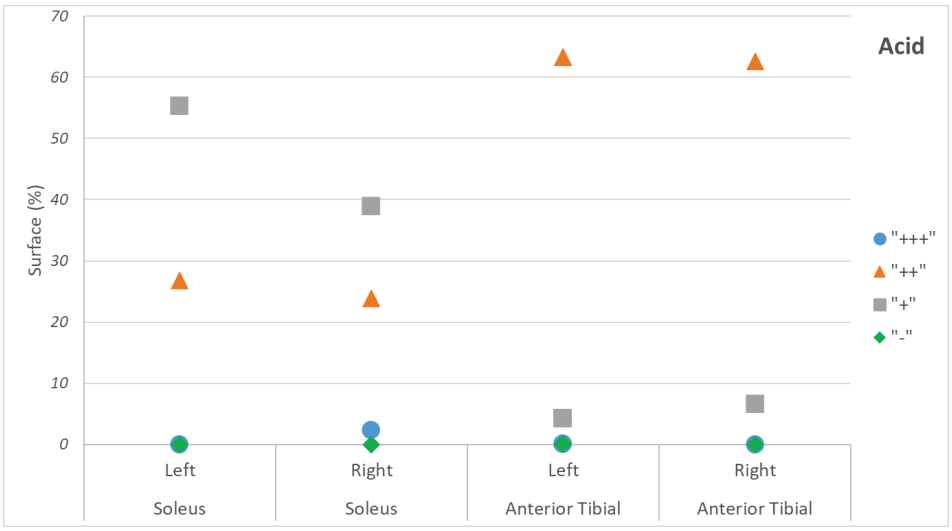

Fig. 9. *Sample mean values for Metamorph surface area in each of the 16 combinations of Muscle, Side, and Intensity in the acid ATPase technique.*

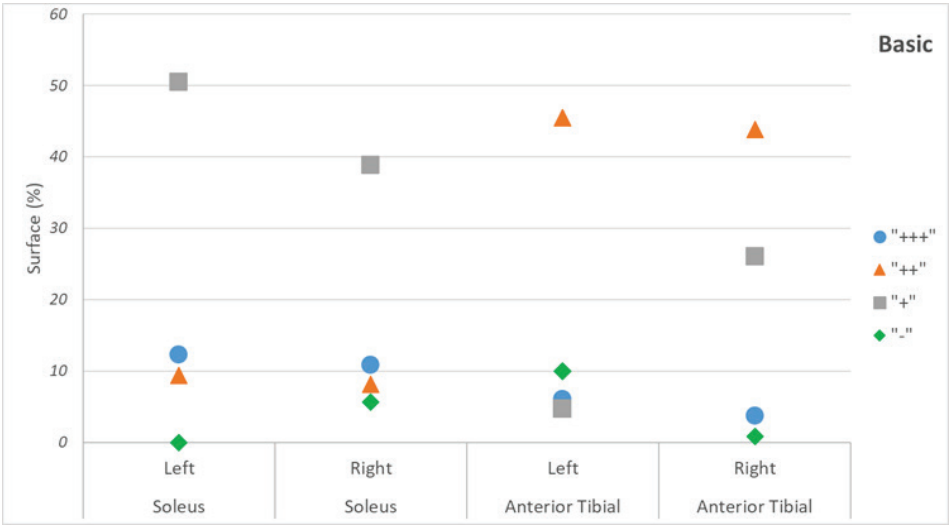

Fig. 10. *Sample mean values for Metamorph surface area in each of the 16 combinations of Muscle, Side, and Intensity in the basic ATPase technique.*

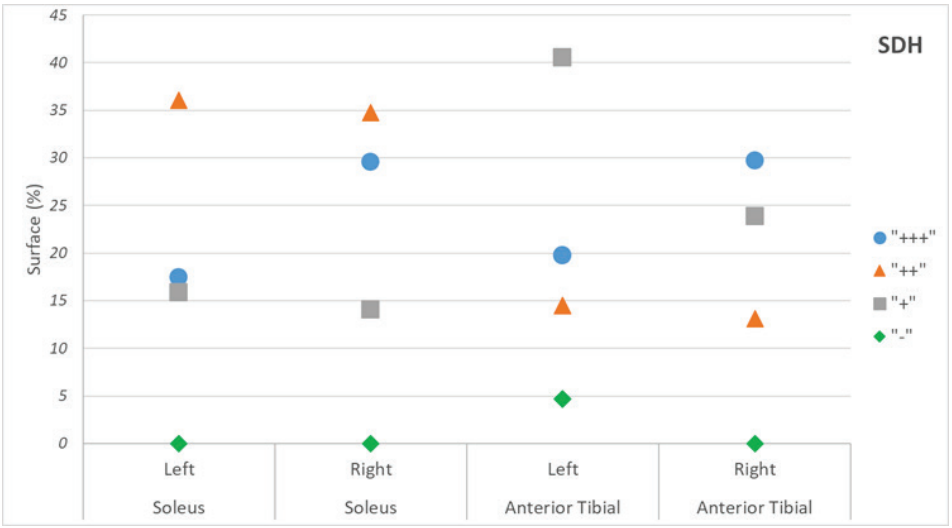

Fig. 11. *Sample mean values for Metamorph surface area in each of the 16 combinations of Muscle, Side, and Intensity in the SDH technique.*

Fig. 11 shows the results of the SDH technique. In this case, the percentages for the highest intensity (+++) were significantly non-zero. Contrary to what was observed in the acid and basic ATPase techniques, in the soleus muscle the average surface area percentage for the moderate intensity (++) was significantly higher than that for the light intensity (+). However, this pattern was reversed in the tibialis anterior muscle, where the average surface area percentage for the light intensity (+) was significantly higher than that for the moderate intensity (++). Fig. 11 also shows that there was no significant difference in average surface area percentages between the left and right soleus muscles across all intensities except the highest (+++). In the tibialis anterior muscle, significant differences were observed between the two sides at the highest (+++) and light (+) intensities.

Histochemical techniques, including acid ATPase, basic ATPase and SDH, show variable results in different types of muscle fibres. Type I (oxidative) fibres often stain intensely with SDH, do not stain with basic ATPase, and show variable staining with acid ATPase. Type II fibres, due to their metabolic variability—which includes both oxidative-glycolytic and glycolytic fibres—present several staining patterns. They are generally stained with basic ATPase, less frequently with acid ATPase, and can often be stained with SDH, although with lower intensity than type I fibres. Fig.s 4a and 5a show type I fibres (oxidative and small in size) intensely stained with SDH in both muscles, whereas type II fibres, oxidative-glycolytic and glycolytic, larger in size, show varying staining intensities. These differences in staining may explain why the areas occupied by fibres stained with ATPase and SDH differ.

There were no quantitative studies with which to compare our results. Studies on muscle fibres and muscles generally provide qualitative information, consisting of individualised observations of fibres in isolated images or data on a small number of fibres, with limited demonstrative value regarding the function of the structure observed. The power of a muscle is determined by the physiological cross-sectional area (PCSA) and the pennation angle. The aim of this work was to provide a method for measuring the PCSA. The soleus and tibialis anterior muscles studied in our work are unipennate fusiform muscles composed of parallel longitudinal fibres. In our study, they were sectioned transversely in their central region of greatest thickness. Due to their location in the hind limb of the rat, they perform their respective functions effectively. The soleus contributes to walking without fatigue, whereas the tibialis anterior is involved in more powerful movements, such as jumping. It should also be noted that muscle power can be increased when more motor units are recruited during activity. A motor unit consists of a motor neuron and the set of muscle fibres it innervates. Our results show that fibrillar composition is related to function: type I (oxidative) muscle fibres predominate in the soleus muscle, which is resistant to fatigue due to its aerobic metabolism, whereas type II (glycolytic and oxidative-glycolytic) fibres predominate in the tibialis anterior. The results of our study, conducted on rat samples, are not directly comparable to humans because of our bipedalism, but they can serve as a basis for future studies or as complementary data.

Observation of the micrographs, such as those presented in this study, shows that the classification of staining intensity into four categories (negative, light, moderate and high) is somewhat imprecise and often questionable when subjectively assigning a section of a fibre to a particular category, as intermediate staining intensities occur between two categories. For this reason, quantification can be affected by human error, mainly in the assessment of the intermediate categories (+) and (++). This potential error arises when using point counting, but not when measuring areas with the Metamorph programme. Therefore, this software can be considered a complementary technique for improving stereological point counting.

ACKNOWLEDGMENTS

To Luis Javier Sánchez Mateos, technician at the Human Histology laboratory, for his help in locating the microscopic slices studied and for his many years of work maintaining and storing them under optimal conditions.

REFERENCES

Appell HJ (1988). Possibility of the transformation of muscle fibers by training and the significance of muscle biopsies for recognizing talent in sports. Sportverletz Sportschaden 2(1): 4-9.

Armstrong RB, Phelps RO (1984). Muscle fiber type composition of the rat hindlimb. Am J Anat 171(3): 259-72.

Bergmeister KD, Gröger M, Aman M, Willensdorfer A, Manzano-Szalai K, Salminger S, Aszmann OC (2017). A Rapid Automated Protocol for Muscle Fiber Population Analysis in Rat Muscle Cross Sections Using Myosin Heavy Chain Immunohistochemistry. J Vis Exp (121): e55441. doi:10.3791/55441.

Brooke MH, Kaiser KK (1970). Muscle fiber types: how many and what kind? Arch Neurol 23(4): 369-79.

Fox J, Garber P, Hoffman M, Johnson D, Schaefer P, Vien J, Zeaton C, Thompson LV (2003). Morphological characteristics of skeletal muscles in relation to gender. Aging Clin Exp Res 15(3): 264-9.

Gorza L (1990). Identification of a novel type 2 fiber population in mammalian skeletal muscle by combined use of histochemical myosin ATPase and anti-myosin monoclonal antibodies. J Histochem Cytochem 38(2):257-65.

Guadilla Y, Benito-Garzón L, Quispe-López N, Montero J (2022). Histologic Outcomes of the Use of Different Biomaterials for Socket Regeneration in Fresh Extraction Sockets: A Split-Mouth Randomized Clinical Trial. Int J Oral Maxillofac Implants 37(5): 1026-36. 10.11607/jomi.9422

Gundersen HJ, Jensen EB (1987). The efficiency of systematic sampling in stereology and its prediction. J Microsc 147(Pt 3): 229-63.

Gundersen HJG, Bagger P, Bendtsen TF, Evans SM, Korbo L, Marcussen N, Møller A, Nielsen K, Nyengaard JR, Pakkenberg B, Sørensen FB, Vesterby A, West MJ (1988). The new stereological tools: disector, fractionator, nucleator and point sampled intercepts and their use in pathological research and diagnosis. APMIS 96(10): 857-81.

Karen P, Stevanec M, Smerdu V, Cvetko E, Kubínová L, Erzen I (2009). Software for muscle fibre type classification and analysis. Eur J Histochem 53(2):87-95. e11 10.4081/ejh.2009.

Konishi M, Iwamoto S, Ohara H, Shimada M (2000). Two-dimensional changes of muscle fiber types in growing rat hind limb. Kaibogaku Zasshi 75(3): 267-73.

Kroustrup JP, Gundersen HJ (1983). Sampling problems in an heterogeneous organ: quantitation of relative and total volume of pancreatic islets by light microscopy. J Microsc 132(Pt 1): 43-55.

Rivero JL, Talmadge RJ, Edgerton VR (1996). Correlation between myofibrillar ATPase activity and myosin heavy chain composition in equine skeletal muscle and the influence of training. Anat Rec 246(2): 195-207.

Ross CD, Meyers RA (2022). Immunohistochemistry of kangaroo rat hindlimb muscles. Anat Rec (Hoboken) 305(6): 1435-47. 10.1002/ar.24791

Santána Pereira JA, de Haan A, Wessels A, Moorman AF, Sargeant AJ (1995). The mATPase histochemical profile of rat type IIX fibres: correlation with myosin heavy chain immunolabelling. Histochem J 27(9): 715-22.

Sawano S, Komiya Y, Ichitsubo R, Ohkawa Y, Nakamura M, Tatsumi R, Ikeuchi Y, Mizunoya W (2016). A One-Step Immunostaining Method to Visualize Rodent Muscle Fiber Type within a Single Specimen. PLoS One 11(11):e0166080. 10.1371/journal.pone.0166080

Schiaffino S, Bormioli SP (1973). Histochemical characterization of adenosine triphosphatases in skeletal muscle fibers by selective extraction procedures. J Histochem Cytochem 21(2): 142-5.

Staron RS, Kraemer WJ, Hikida RS, Fry AC, Murray JD, Campos GE (1999). Fiber type composition of four hindlimb muscles of adult Fisher 344 rats. Histochem Cell Biol 111(2): 117-23.